Advances in Science and Technology Research Journal

Advances in Science and Technology Research Journal, 2026, 20(2), 361–373
https://doi.org/10.12913/22998624/211152
ISSN 2299-8624, License CC-BY 4.0

Received: 2025.10.15
Accepted: 2025.08.30
Published: 2025.12.23

Numerical and analytical methods for calculating the buckling load of a carbon-epoxy beam using Digimat software

Jarosław Gawryluk[1*], Grażyna Ryzińska[2], Wiesław Frącz[2]

[1] Department of Applied Mechanics, Lublin University of Technology, Nadbystrzycka 36, 20-618 Lublin, Poland
[2] Department of Materials Forming and Processing, Rzeszow University of Technology, Powstańców Warszawy 8, 35-959 Rzeszów, Poland
* Corresponding author's e-mail: j.gawryluk@pollub.pl

ABSTRACT

The aim of this work was to evaluate the effectiveness of the homogenisation process using the layered composites made of carbon-epoxy prepregs subjected to compression. A rectangular cross-section cantilever beam loaded with a compressive force at its free end was subjected to detailed analysis. On the basis of the Digimat software, the material constants of the prepreg and the substitute engineering constants for the entire composite structure consisting of various numbers of layers (8–16 layers) were determined. The obtained material constants were used in analytical (Euler) and numerical (finite element method) studies. Three models were developed in the Abaqus software: a shell and solid model for the layered composite and a homogeneous shell model with orthotropic properties. The critical force at which the structure buckles was determined. A high degree of agreement (above 95%) was obtained between the substitute material model and the theoretical results and the solid model.

Keywords: Euler's formula, critical force, homogenisation, Digimat, finite element method.

INTRODUCTION

Composite materials, particularly carbon fiber reinforced polymers (CFRPs), are widely used in lightweight structural applications due to their excellent strength-to-weight ratio and tailored mechanical properties. In structural design, one of the key challenges is ensuring stability under compressive or axial loads, where slender elements are prone to buckling. Accurate prediction of the critical load, beyond which sudden instability may occur, is essential for safe and efficient design.

Identifying the mechanical properties of a composite material is a key stage in the design process. These properties depend on the internal structure of the material, including the topology and geometry of the composite, as well as the material constants of its components. In unidirectional prepregs, two phases can be distinguished: the matrix and the reinforcement. The matrix is resin (the most commonly used in industry is epoxy resin [1]), while the reinforcement is fibres arranged in one direction, i.e. continuous, long fibres [2–3]. Depending on the diameter of the carbon fibres and their volume in the laminate, the properties of the entire prepreg change. Since fibres are the main load-bearing component of the composite, a high fibre volume fraction (V_f) has a positive effect on the mechanical properties of the composite. However, the percentage of reinforcement cannot be overdone, as volume fractions higher than 60% result in poor wettability and infiltration of the matrix material into the fibres [4]. The theoretical fibre volume limit is determined by the cylindrical shape of the fibre, while the practical limit is determined by processing limitations and the ability of the matrix to transfer loads to and from the fibres. The resin volume must be sufficient to minimise voids in the laminate. Voids are stress concentrators and reduce the final strength of the laminate, so their presence is not desirable. For prepregs used in the aerospace industry, typical V_f values range from 50 to 60%.

Analytical and numerical methods are helpful in properly designing the properties of a prepreg before it is manufactured. Several analytical micromechanical models are available to predict the effective elastic properties of composite materials. The classical models proposed by Voigt [5] and Reuss [6] set the upper and lower limits of these estimates. In addition, the Mori-Tanaka model [7–9] focuses on evaluating the average internal stress in a matrix containing inclusions, using the concept of intrinsic deformation. Below is an overview of research papers presenting available methods in the context of carbon laminate simulation. In [10], the authors compared different methods of homogenising the mechanical properties of CFRP composites, such as the Voigt, Reuss, Mori-Tanaka and Method of Cells (MOC) [11–12], as well as FEM numerical analysis using a representative volume element (RVE) in the Abaqus software [13]. A carbon laminate in an epoxy matrix with a fibre content of 62% was analysed. The numerical model consisted of unidirectional cylindrical fibres periodically arranged in a polymer matrix to reproduce the cross-section. Periodic Boundary Conditions (PBCs) were applied, which allowed for the continuity of displacements between opposite RVE walls, simulating an unlimited, repeatable material structure. The Voigt and Reuss models only provided limit values, while the Mori-Tanaka and MOC models showed high consistency with both FEM simulation results and experimental data. These models predicted longitudinal, transverse and shear moduli with a deviation of less than 5% from the experimental values, indicating their high accuracy in the analysis of the structural properties of CFRP composites. The authors of [14] presented a new algorithm for generating representative volume elements (RVE) with random fibre distribution, which statistically reflects the actual microstructure of fibre-reinforced composites. The generated structures were compared with the actual structure, showing high consistency. On the basis of the developed RVEs, finite element simulations (Abaqus) were performed to determine the effective elastic properties of carbon prepreg. The results showed very good agreement for the longitudinal modulus, while the values for the transverse direction were slightly underestimated. In article [15], a new method of probabilistic analysis of the elastic properties of unidirectional carbon composites was proposed, based on a micromechanical model of theory and Monte Carlo simulation. The authors compared various commonly used micromechanical models (including the rule of mixtures, Halpin–Tsai, and bridging models) to determine the deterministic properties of the composite. The bridging model proved to be the best. In addition, a sensitivity analysis was performed, which showed that E_1 is most influenced by the fibre modulus and fibre volume fraction, E_2 by the fibre fraction, whereas matrix properties, and G_{12} by the fibre fraction and matrix parameters. The paper [16] presented an advanced numerical homogenization methodology for predicting the mechanical properties of polymer composites based on their microstructure. The composites containing spherical particles and fibres were studied using RVE in finite element analysis. An innovative approach to three-dimensional boundary conditions, especially periodic ones, was developed, which significantly improved the accuracy of the simulation. The results were compared with experimental data and classical analytical models (such as Mori-Tanaka or Double Inclusion), achieving good agreement. The article [17] presented new analytical models predicting effective Young's moduli and shear strength in carbon composites, taking into account the material, layer orientation and thickness. The authors proposed an original K-PY algorithm consisting of three main steps: (1) calculating the elastic properties of the components (fibres and matrix) using the Chamis model; (2) obtaining the stiffness matrix of each layer by volume averaging; (3) optimizing the results using an objective function to obtain properties closest to the experiment. Good parameter agreement (up to 5%) was obtained. Katouzian et al. [18] proposed an effective method for calculating the homogenised mechanical properties of fibre-reinforced epoxy matrix composites, assuming that the material can be treated as elastic and transversely isotropic. The model was based on the use of the finite element method (FEM) to calculate the stress and strain field in a representative volume element (RVE), followed by the use of the least squares method to obtain the most reliable values of elastic constants. In article [19], a multiscale analysis of the mechanical properties of flat-woven fabric composites reinforced with carbon fibres and an epoxy matrix was conducted. The research included homogenisation of the material microstructure to determine

the effective elastic properties and the use of Monte Carlo simulation to account for material uncertainties at the micro and macro levels. The results were compared with mixture theory and experimental data, confirming the effectiveness of the method used. In addition, a sensitivity analysis was performed, which showed that the mechanical properties are most influenced by the parameters of the carbon fibres and the matrix.

Material models obtained by homogenisation are a practical tool in the engineering analysis of carbon composite structures. Homogenisation makes it possible to replace the complex microstructure of a composite with a homogeneous medium with effective mechanical properties. The material data simplified in this way can be directly used in classic engineering calculations, such as the analysis of composite beam deflection or the estimation of the critical force of load-bearing structures. This method reduces the time required for numerical calculations [20] and allows for high accuracy in predicting the behaviour of structures, especially when the appropriate directions of anisotropy, both in-plane and out-of-plane, are taken into account. In engineering practice, this allows for the design of lightweight and durable CFRP components with greater certainty regarding their load-bearing capacity and stiffness.

Modern multiscale modelling tools, such as Digimat, enable detailed assessment of the effective properties of composites based on microstructural parameters. These unified properties can then be used in finite element models to analyse the global response of structures. Many scientific publications used Digimat to model various types of composites, including ceramics [21], WPC composites [22], carbon composites [23–24] and natural composites [25–26]. In [27], the authors tested two methods of modelling material in the Digimat software: MF (Mean Field) and FE (Finite Element), using carbon-epoxy fabrics as an example. The results of numerical modelling were compared with experimental samples. It was found that the largest error (approx. 14%) between the simulation and the actual experiment was obtained for the Digimat FE model, while the simpler Digimat MF model yielded the smallest difference of 0.5%. In summary, Digimat is a useful tool for modelling layered composites, because it allows for accurate prediction of how different layers affect the properties of the entire composite structure. This helps to better understand the behaviour of composites under load and to design them to be more durable and efficient. This work aimed to present the capabilities of Digimat and demonstrate how it can assist in the analysis and design of composites.

The buckling of laminated composite plates has been extensively studied within the framework of the classical laminate theory (CLT), which combines Classical Plate Theory with lamination theory to predict in-plane stiffness, bending stiffness, and coupling effects. However, CLT neglects transverse shear deformation, which can lead to discrepancies for moderately thick laminates or when shear effects are significant. To address this limitation, refined models such as the first-order shear deformation theory (FSDT) and various higher-order shear deformation theories (HSDT) have been developed [28]. More recently, finite element methods have become the standard tool for analysing buckling in laminated structures, enabling the consideration of realistic layups, boundary conditions, and geometric nonlinearities. In [29], the authors presented the results of compressive analytical and numerical tests of beams with different cross-sections made of polymer composites. An interesting direction of research are modern structures made of natural laminates. Numerical studies of various configurations of composite angles were presented in [30]. The first modes of buckling under axial compression of a simply supported column made of flax prepreg were analysed.

This paper analysed the buckling of a carbon fibre composite beam. The novelty is combining Euler's method for determining the critical load, Mori-Tanaka homogenisation, and finite element method (FEM) analysis to demonstrate that a simplified homogenised model can effectively replace a full layered model in buckling analysis. Using Digimat software, the multilayer composite structures were homogenised and the effective stiffness parameters were calculated as a function of the elastic properties of the fibre and matrix. Next, a cantilever beam with different material properties was modelled in the Abaqus environment (detailed model: laminate; simplified model: homogeneous structure). The critical load at which the system loses stability was determined using the FEM.The numerical results were compared with the classical theory of laminates using Euler's theory to assess the accuracy of material property homogenisation in the context of composite structures.

HOMOGENISATION OF MATERIAL

The work used the Digimat MF module. It uses Eshelby-based semi-analytical mean-field homogenisation approaches and an analytical description of the material in order to compute the thermo-mechanical, thermal or electrical properties of a composite as a function of its microstructure morphology, i.e., inclusion shape, orientation, volume/mass fraction, and micro, i.e., per-phase, material behaviour.

The material data for the fibre and resin in the elastic range were taken from publication [31] (Table 1–2). The reinforcement material was modelled as elastic, with transverse isotropy, while the resin material was modelled as isotropic. On this basis, a composite layer model was constructed based on a RVE with a reinforcement volume fraction of 50%. The next step was homogenization according to the selected scheme.

A simplified fibre geometry was adopted, with a circular cross-section. The fibres in the unit cell of a single composite layer were arranged in one direction. These were continuous fibres, not bonded in the transverse direction, with diameters given in Table 1. The fibre distribution was random with respect to position, maintaining mutual parallelism (Figure 1). The free spaces between the carbon fibres were completely filled with resin. Consequently, the volume fractions of the composite components were the same.

The homogenization of composites in Digimat-MF takes place in two stages. The actual composite RVE is replaced by a model RVE, which is an aggregate of so-called pseudo-grains. Each pseudo-grain occupies a specific domain and is a basic two-phase composite consisting of a phase that is a matrix reinforced with identical and aligned inclusions with appropriate orientation. The homogenisation of the model RVE (Figure 1) takes place in two stages. First, each pseudo-grain is homogenised using the MFH (Mean Field Homogenization) model appropriate for basic two-phase composites (in this work, the Mori-Tanaka first order model was used). Then, the effective response of the set of homogenised pseudo-grains is calculated. In this second stage, the Voigt model is used, which gives good results, especially in the most common case of N = 1 (i.e., one inclusion family). A view of the unit cell of the tested composite is shown in Figure 1. The calculations allowed the mechanical properties of a single layer for the tested laminate to be determined (Table 3).

In the next step, a representative volume element (RVE) model was created, reflecting the composite layer arrangement in a given fibre orientation sequence (Table 4). Each layer was treated as a separate phase with specific micromechanical properties (Tables 1–2). The reinforcement filling covered 50% of the layer. The model assumed perfect bonding between layers, no porosity, and uniform fibre distribution in each

Table 1. Material properties of the carbon fibre T700 [31]

Parameter	Sample	Unit	T700
Density	ρ_f	kg/m^3	1800
Fibre diameter	d_f	m	0.00000762
1-direction tensile modulus	E_{f1}	Pa	230000000000
2-direction tensile modulus	E_{f2}	Pa	18000000000
12- direction shear modulus	G_{f12}	Pa	8700000000
23- direction shear modulus	G_{f23}	Pa	5800000000
12-direction Poisson's ratio	v_{f12}	-	0.2
23-direction Poisson's ratio	v_{f23}	-	0.49

Table 2. Material properties of the epoxy resin AF-426A/B [31]

Parameter	Sample	Unit	AF-426A/B
Density	ρ_m	kg/m^3	1200
Tensile modulus	E_m	Pa	3000000000
Shear modulus	G_m	Pa	1250000000
Poisson's ratio	v_m	-	0.33

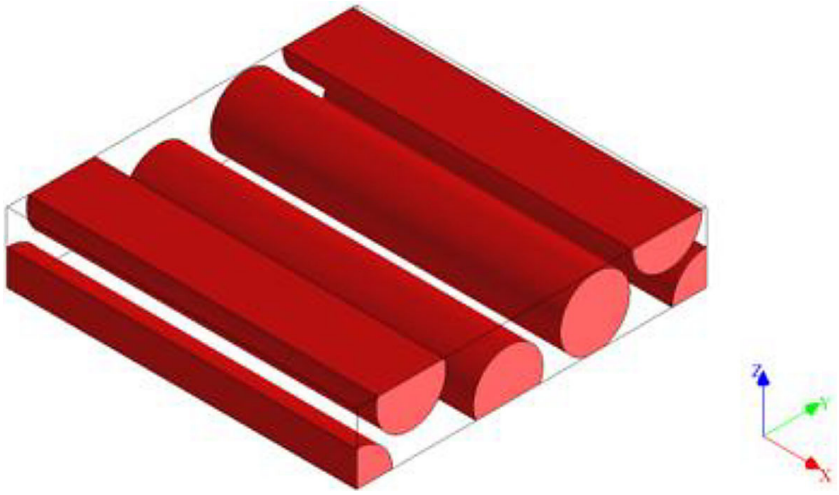

Figure 1. View of the RVE

Table 3. Calculated engineering constants for the layer of the tested composite

Parameter	Sample	Unit	Composite
Density	ρ_c	kg/m^3	1500
1-direction tensile modulus	E_{c1}	Pa	116520000000
2-direction tensile modulus	E_{c2}	Pa	6377000000
12- direction shear modulus	G_{c12}	Pa	2277000000
23- direction shear modulus	G_{c23}	Pa	2541000000
12-direction Poisson's ratio	v_{c12}	-	0.399
23-direction Poisson's ratio	v_{c23}	-	0.418

layer. Five configurations with different structure thicknesses in the range of 0.4–0.8 mm were considered. The thickness of a single composite layer was 0.05 mm.

All analysed cases contained an even number of layers, the distribution of which was symmetrical with respect to the reference plane. As a result of the homogenisation of the entire composite, the results were obtained in the form of a compliance matrix. Sample values for the [0/30/-30/90]s configuration are shown in Figure 2.

The compliance matrices obtained for composite structures with a given layer arrangement allowed determining the resultant engineering constants (Table 5) based on well-known relations from composite mechanics [32] concerning the general theory of anisotropic elasticity (Equation 1):

$$\begin{Bmatrix} \varepsilon_1 \\ \varepsilon_2 \\ \varepsilon_3 \\ \gamma_{23} \\ \gamma_{13} \\ \gamma_{12} \end{Bmatrix} = \begin{bmatrix} S_{11} & S_{12} & S_{13} & S_{14} & S_{15} & S_{16} \\ S_{21} & S_{22} & S_{23} & S_{24} & S_{25} & S_{26} \\ S_{31} & S_{32} & S_{33} & S_{34} & S_{35} & S_{36} \\ S_{41} & S_{42} & S_{43} & S_{44} & S_{45} & S_{46} \\ S_{51} & S_{52} & S_{53} & S_{54} & S_{55} & S_{56} \\ S_{61} & S_{62} & S_{63} & S_{64} & S_{65} & S_{66} \end{bmatrix} \times \begin{Bmatrix} \sigma_1 \\ \sigma_2 \\ \sigma_3 \\ \tau_{23} \\ \tau_{13} \\ \tau_{12} \end{Bmatrix} \quad (1)$$

where: $\varepsilon_1,\varepsilon_2,\varepsilon_3$ – normal strains in the directions of the principal axes of the material, $\gamma_{23},\gamma_{13},\gamma_{12}$ – shape strains (angular) in the respective planes, $\sigma_1,\sigma_2,\sigma_3$ – normal stresses, $\tau_{23},\tau_{13},\tau_{12}$ – shear stresses. The S_{ij} coefficients contain information about the susceptibility of the material to deformation under a specific type of stress.

For an orthotropic material such as carbon prepreg, some terms of the compliance matrix are 0. The remaining terms can be transformed as follows:

$$\begin{gathered} E_1 = \frac{1}{S_{11}};\ E_2 = \frac{1}{S_{22}};\ E_3 = \frac{1}{S_{33}} \\ \nu_{12} = -\frac{S_{12}}{S_{11}};\ \nu_{13} = -\frac{S_{13}}{S_{11}};\ \nu_{23} = -\frac{S_{23}}{S_{22}} \\ G_{12} = \frac{1}{S_{66}};\ G_{13} = \frac{1}{S_{55}};\ G_{23} = \frac{1}{S_{44}} \end{gathered} \quad (2)$$

where: E_1,E_2,E_3 – Young's moduli,
$\nu_{12},\nu_{13},\nu_{23}$ – Poisson's ratios,
G_{12},G_{13},G_{23} – Kirchhoff's moduli.

Table 4. Analysed configurations of composite layer arrangement

Case	Configuration
C1	[0/30/-30/90]s
C2	[0/-30/30/90/0]s
C3	[0/30/-30/90/0/90]s
C4	[0/60/-60/45/-45/90/0]s
C5	[0/0/45/-45/90/90/0/0]s

ANALYTICAL STUDY

Composite laminates, due to their layered structure, are characterised by strong anisotropy of mechanical properties. Therefore, CLT is used for their analysis, which allows the effective properties of the entire laminate cross-section to be determined based on the properties of individual layers [32]. In the analysis of laminates, a simplified, orthotropic form of the elastic stiffness matrix (in the 1–2 plane) is usually used:

$$\begin{bmatrix}\sigma_1\\ \sigma_2\\ \tau_{12}\end{bmatrix} = \begin{bmatrix}Q_{11} & Q_{12} & 0\\ Q_{12} & Q_{22} & 0\\ 0 & 0 & Q_{66}\end{bmatrix} \times \begin{bmatrix}\varepsilon_1\\ \varepsilon_2\\ \gamma_{12}\end{bmatrix} \quad (3)$$

where: Q_{ij} – stiffness matrix terms.

In this case, a cantilever beam with a rectangular cross-section (Figure 3) composed of many thin layers oriented at different angles to the main axis is considered (according with cases presented in Table 4).

Compliance matrix

	11	22	33	12	23	13
11	1.6268E-005	-5.4935E-006	-5.8928E-006	6.929E-022	3.8447E-021	-2.4087E-020
22	-5.4935E-006	2.817E-005	-1.064E-005	-3.5075E-021	-1.9905E-020	1.5614E-022
33	-5.8928E-006	-1.064E-005	0.00013697	1.1765E-021	5.9574E-021	8.353E-021
12	6.929E-022	-3.5075E-021	1.1765E-021	7.8494E-005	-2.4181E-020	-1.2972E-022
23	3.8447E-021	-1.9905E-020	5.9574E-021	-2.4181E-020	0.00042078	-6.1205E-022
13	-2.4087E-020	1.5614E-022	8.353E-021	-1.2972E-022	-6.1205E-022	0.00040942

Figure 2. Example of a compliance matrix obtained from the Digimat-FM module for a composite structure with C1 configuration

Table 5. Calculated engineering constants for the tested structures

Parameter		C1	C2	C3	C4	C5
E1	[Pa]	61470370000	72516320000	62656640000	43084880000	67069080000
E2	[Pa]	35498760000	30165910000	44662800000	43103450000	40128410000
E3	[Pa]	7300870000	7266390000	7314750000	7322790000	7304600000
v12	[-]	0.34	0.34	0.20	0.33	0.23
v13	[-]	0.36	0.38	0.42	0.33	0.42
v23	[-]	0.38	0.39	0.41	0.33	0.41
G12	[Pa]	2442480000	2462210000	2431490000	2409520000	2442480000
G13	[Pa]	2376540000	2356710000	2387550000	2409520000	2376540000
G23	[Pa]	12740480000	10700910000	9340560000	16139440000	9340560000

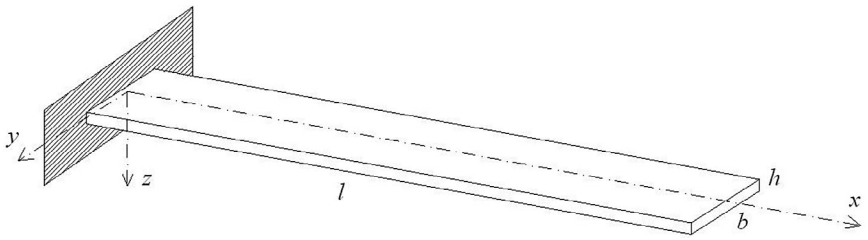

Figure 3. The composite beam shape

Using the material data specified for carbon prepreg based on the MF model from Digimat (Table 3), the stiffness matrix [*Q*] of the layer oriented in the *0* direction (x-axis) was determined using Equation 4:

$$[Q] = \begin{bmatrix} \frac{E_1}{D_Q} & \frac{E_2\nu_{12}}{D_Q} & 0 \\ \frac{E_2\nu_{12}}{D_Q} & \frac{E_2}{D_Q} & 0 \\ 0 & 0 & G_{12} \end{bmatrix} \quad (4)$$

where: $D_Q = 1 - \frac{E_2}{E_1}\nu_{12}^2 = 1 - \nu_{21}\nu_{12}$

Then, using the matrix values for layer 0, the matrices for individual layers at any angle θ were determined using Equations 5:

$$\begin{gathered} \bar{Q}_{11} = Q_{11}cos^4\theta + 2(Q_{12} + 2Q_{66}) \\ sin^2\theta\, cos^2\theta + Q_{22}sin^4\theta \\ \bar{Q}_{12} = (Q_{11} + Q_{22} - 4Q_{66}) \\ sin^2\theta\, cos^2\theta + Q_{12}(sin^4\theta + cos^4\theta) \\ \bar{Q}_{22} = Q_{11}sin^4\theta + 2(Q_{12} + 2Q_{66}) \\ sin^2\theta\, cos^2\theta + Q_{22}cos^4\theta \\ \bar{Q}_{16} = (Q_{11} - Q_{12} - 2Q_{66})sin\theta\, cos^3\theta + \\ +(Q_{12} - Q_{22} - 2Q_{66})sin^3\theta\, cos\theta \\ \bar{Q}_{26} = (Q_{11} - Q_{12} - 2Q_{66})sin^3\theta\, cos\theta \\ +(Q_{12} - Q_{22} - 2Q_{66})sin\theta\, cos^3\theta \\ \bar{Q}_{66} = (Q_{11} + Q_{22} - 2Q_{12} - 2Q_{66}) \\ sin^2\theta\, cos^2\theta + Q_{66}(sin^4\theta + cos^4\theta) \end{gathered} \quad (5)$$

In the analysis of laminates, the next step is to determine the disc stiffness matrix *[A]* of the entire laminate, which takes into account the influence of all layers and their orientation relative to each other, using Equation 6:

$$A_{ij} = \sum_{n=1}^{n} \left(\bar{Q}_{ij}\right)_n (z_n - z_{n-1}) \quad (6)$$

where: *n* is the total number of layers in the laminate, $\overline{Q_{ij}}$ are the elements of the stiffness matrix of the n-th layer, z_n is the distance from the reference plane to the surface of the n-th layer (Figure 4).

Then, using the first term of matrix A11, the effective Young's modulus of the laminate along the main axis was calculated [33]:

$$\mathrm{E}_{eff} = \frac{A_{11}}{h} \quad (7)$$

The determined effective Young's modulus was used to determine the critical force of the structure subjected to compressive force using Euler's formula [34]:

$$\mathrm{F}_{cr} = \frac{\pi^2 E_{eff} J}{(\mu L)^2} \quad (8)$$

where: F_{cr} – bifurcation force, E_{eff} – effective Young's modulus, J – minimal area moment of inertia of the cross section,
μ – beam effective length factor (for the case of a cantilever beam equal 2),
L – length of the beam.

NUMERICAL MODEL

Numerical studies were conducted for the cantilever beam shown in Figure 3. A buckling analysis was performed in the Buckling module, which resulted in the value of the force corresponding to the first mode of buckling. The finite element method was used in the Abaqus software, where five different configurations were analysed (Table 4). The data flow between Digimat (material homogenization), Abaqus (FEM analysis) and classical laminate theory (analytical study) is presented in Figure 5.

A system with a length of 300 mm and a width of 30 mm was subjected to a detailed analysis. This maintains a balanced length to width ratio (L/b=10), which is within the typical range for beam elements and allows for conducting a buckling analysis without the dominance of local phenomena. The thickness of the tested element resulted from the definition of the configuration of layers with a specified single layer thickness of 0.05 mm.

Three numerical models of the analysed structure were prepared in the Abaqus software. In the first model of thin-walled structures (Figure 6a), S8R shell elements were used. These are 8-node shell elements of the second order, which have six degrees of freedom in each node (displacements and rotations). The second variant used SC8R elements, which are solid, 8-node continuum shell elements (Figure 6b). Each node of the element has 3 translational degrees of freedom. In both models, the layer configurations were defined using the Layup-Ply technique, with which each layer was assigned the appropriate thickness, fibre orientation and material constants defined in Table 3. The third model was made of S8R shell elements

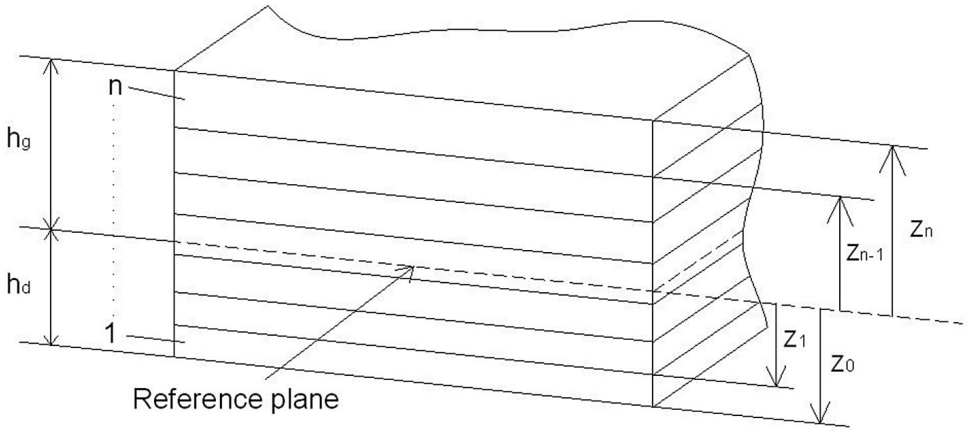

Figure 4. Distances layers from the reference plane

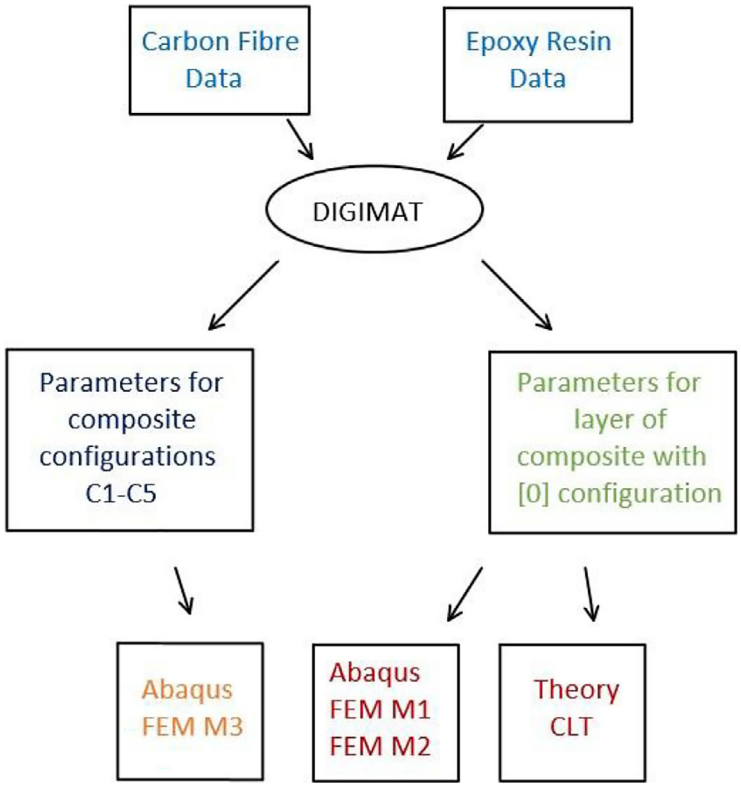

Figure 5. Diagram illustrating the data flow during calculations

(Figure 4a), while the layer arrangement of composite structures was not modelled. Instead, the material description specified in the Digimat simulation was used (Table 5). In addition, the structure was defined as homogeneous with a thickness corresponding to the total thickness of the compressive element.

Each of the analysed models was identically loaded with an axial force of 1N at one end of the beam, directed along the beam. The opposite end of the beam was blocked in all directions, simulating full wall restraint.

COMPARISON ANALYSIS

After conducting analytical and numerical studies, a comparative analysis of the results obtained for all configuration cases was performed. Table 6 presents the critical force results obtained for the first buckling mode (Figure 7). Relative errors were calculated between the obtained results based on the following relationships: $Error1 = ((F_{M3}-F_T)/F_{M3}) \times 100\%$; $Error2 = ((F_{M3}-F_{M1})/F_{M3}) \times 100\%$; $Error3 = ((F_{M3}-F_{M2})/F_{M3}) \times 100\%$. The reference model for calculating the

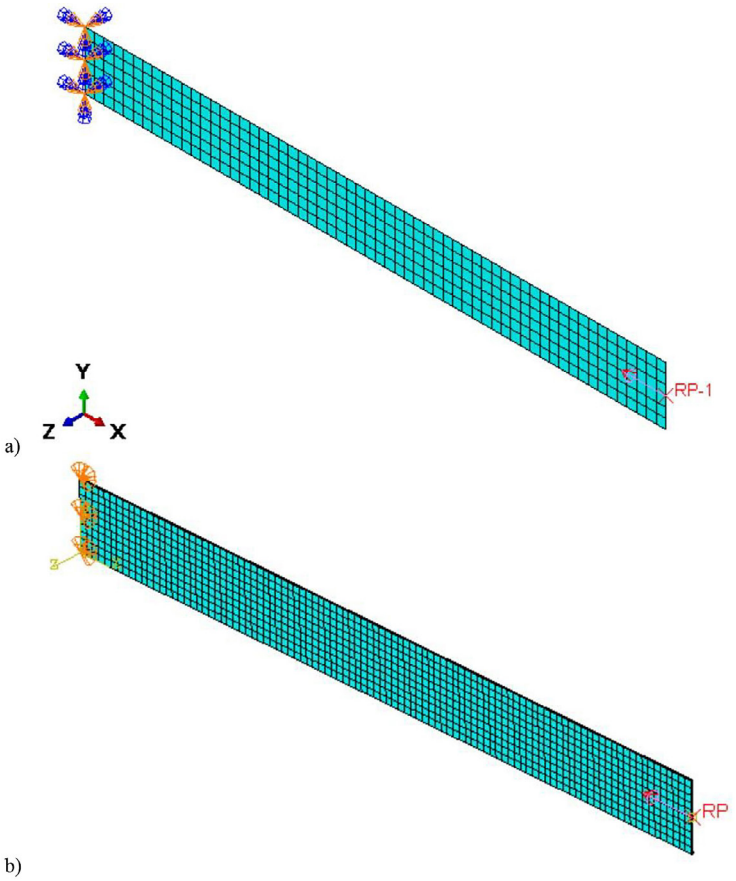

Figure 6. Numerical models of the analysed structures: a) shell, b) solid

above-mentioned errors is FEM M3. The aim was to demonstrate the differences in the context of the simplified model.

After analysing the results, it was found that the structure model using homogenised material (M3) obtained values similar to those of model M2 (the relative error for each configuration was below 5%) and analytical calculations (relative error between 2–11% depending on the layer configuration). On the other hand, the shell model, in which composite layers were modelled (M1), achieved the highest stiffness for each configuration (Figure 8). The largest difference between the M3 substitute model and the M1 model was observed for configuration C1 (approx. 37%). Overall, the M1 model exhibits the highest bifurcation force among the models considered, even exceeding the value predicted by classical laminate theory (CLT). These differences result primarily from the kinematics adopted in the shell element and the full consideration of the layer arrangement, including the surface layers [0], which have the greatest influence on bending stiffness. Simplified shell assumptions limit through-thickness shear strain, which also contributes to

Table 6. Bifurcation force results for all configurations and errors obtained

Parameter	Bifurcation force [N]				
Case	C1	C2	C3	C4	C5
Theory	0.290	0.650	0.950	1.130	2.420
FEM M1	0.371	0.690	1.150	1.169	2.690
FEM M2	0.284	0.632	0.957	1.030	2.390
FEM M3	0.271	0.622	0.929	1.019	2.358
Error1	-7.010	-4.500	-2.260	-10.890	-2.630
Error2	-36.900	-10.930	-23.790	-14.720	-14.080
Error3	-4.800	-1.610	-3.010	-1.080	-1.360

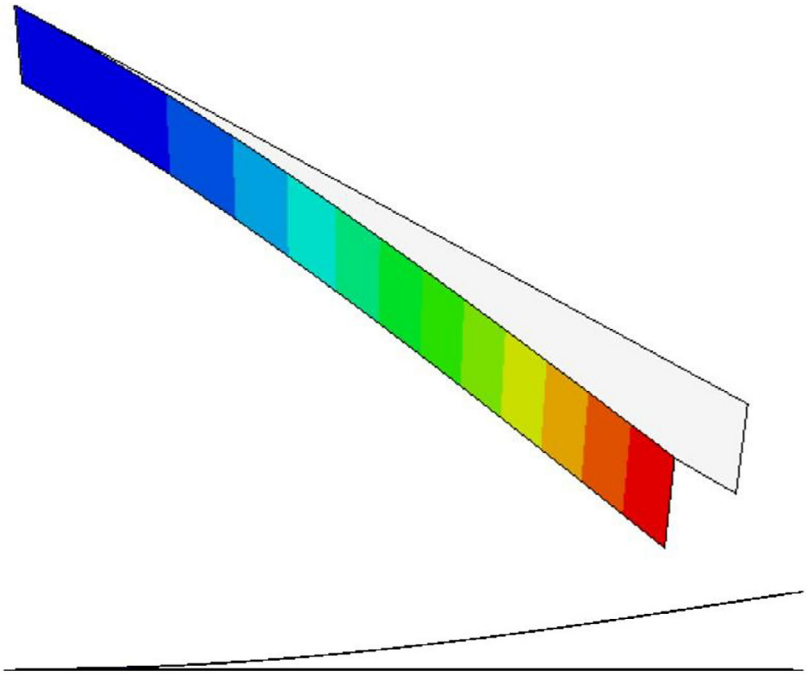

Figure 7. The first buckling mode

increased stiffness. The M2 model allows for full 3D deformations, including through-thickness shear and tension, which reduces the effective stiffness and produces a result similar to CLT theory. On the other hand, the shell with equivalent properties (M3) treats the laminate as a homogeneous orthotropic cross-section, the properties of the surface layers are not taken into account, therefore the obtained results are closer to the theory than to the M1 model. In addition, it was observed globally for all models that as the number of layers in the composite structure increased, the stiffness of the structure also increased (Figure 9). Moreover, using the M3 model as an example, it was found that adding two additional layers in the centre of the composite in the [0] direction (the difference between C1–C2) increased the stiffness of the system by 129%. Furthermore, including two additional layers in the [90] direction (the difference between C2–C3) increased the stiffness by 49%. The system is very sensitive to the direction of the layers.

In addition, the theoretical results were compared with the FEM models (Figure 10). Relative

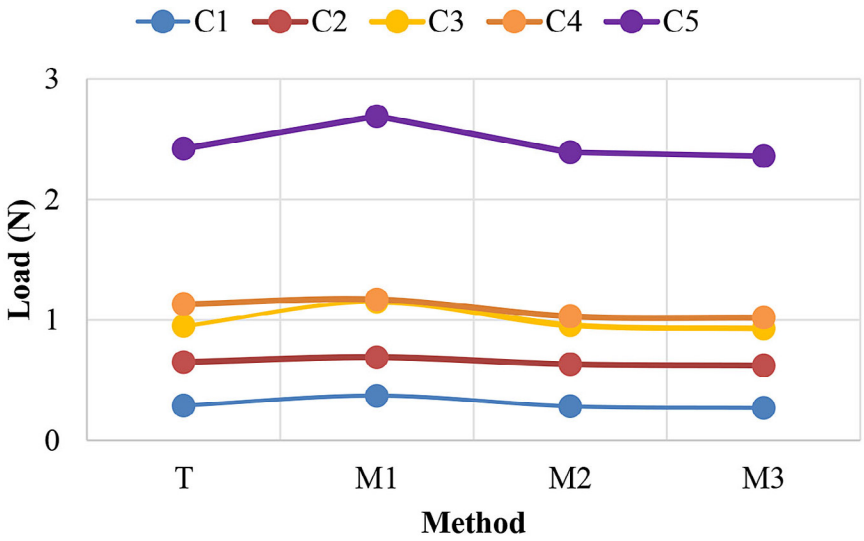

Figure 8. Bifurcation load of cantilever beam for different method

Figure 9. Relative errors calculated for all configurations

Figure 10. Relative errors with respect to theoretical results for five configurations

errors were calculated on the following relationships: $Error4 = ((F_T\text{-}F_{M1})/F_T) \times 100\%$; $Error5 = ((F_T\text{-}F_{M2})/F_T) \times 100\%$; $Error6 = ((F_T\text{-}F_{M3})/F_T) \times 100\%$. The largest differences in results between the theoretical analysis and FEM models were obtained for the M1 shell model. A similar tendency was obtained for all configurations, except case C4. In this case, the M1 model achieved the highest compliance with CLT (3.5%). However, the remaining models (M2 and M3) achieved the highest differences in this case, approximately 9% and 10%, respectively.

The level of agreement between the FEM models and CLT strongly depends on the laminate configuration. The possible reasons for this include the significant contribution of surface plies and the effective in-plane stiffness. In authors' view, the role of laminate symmetry or orthotropic coupling is less important, since all configurations considered are symmetric and, as a result, such couplings remain inactive.

CONCLUSIONS

This paper presented analytical and numerical studies of the compression of a cantilever beam made of carbon prepreg in various layer configurations. The main objective was to verify the effectiveness of modelling a substitute material for a composite with any layer configuration in the Digimat software. The first-order Mori-Tanaka homogenisation model was used, assuming 50% carbon fibre filling and 50% epoxy resin in a single prepreg layer. Determining the substitute properties of the entire composite structure enabled simple

FEM modelling of the structure as a homogeneous solid with orthotropic properties. The results obtained for five different configurations (with different structure thicknesses) were compared with the models in which all layers were determined separately using the Layup-ply technique. In addition, the classical theory of laminates was used to determine the effective Young's modulus of the structure, which allowed the critical force of the structure to be determined based on Euler's formula. High consistency of theoretical results with numerical models (M2 and M3) was achieved, with relative error ranging from -1% to 10% depending on the configuration. For the configuration [0/60/-60/45/-45/90/0]s, it was found that the results of model M1 were closest to the theory (error below 4%). In the other configurations, a large discrepancy in the results was observed (maximum difference of approximately 28%). Different stacking sequences exhibit varying stiffness, anisotropy, and coupling between directions, which affect how accurately the classical laminate theory captures the actual behaviour of the laminate. On the other hand, the finite element method accounts for a more complete field of displacements and stresses. In authors' opinion, this is the reason why the discrepancy between FEM and CLT results varies depending on the stacking sequence.

The proposed replacement model M3 also achieved high consistency of results with the solid model M2 (minimum consistency 95%) for all configurations. However, between the M3 model and the theoretical results, high agreement was obtained for cases C2, C3, and C5 (agreement above 95%) and slightly worse agreement of results for models C1 (approx. 93%) and C4 (approx. 89%). Using the Digimat software, it was found that the thickness of a single laminate layer does not affect the considered material properties (engineering constants). An important factor is the volume of fibre filling in the layer, which, according to scientific literature, is usually assumed to be in the range of 50–60% for layered composites.

Acknowledgements

The research leading to these results has received funding from the commissioned task entitled "VIA CARPATIA Universities of Technology Network named after the President of the Republic of Poland Lech Kaczyński" under the special purpose grant from the Minister of Education and Science, contract no. MEiN/2022/DPI/2575, as part of the action "In the neighborhood – inter-university research internships and study visits".

REFERENCES

1. Somarathna Y., Herath M., Epaarachchi J., Islam M.M. Formulation of epoxy prepregs, synthesization parameters, and resin impregnation approaches – a comprehensive review. *Polymers* 2024; *16*: 3326. https://doi.org/10.3390/polym16233326
2. Kowal M., Pietras D. Carbon fibre reinforced polymer fatigue strengthening of old steel material. Advances in Science and Technology Research Journal. 2023; 17(1): 197–209. https://doi.org/10.12913/22998624/156216
3. Kowal M. Effect of adhesive joint end shapes on the ultimate load-bearing capacity of carbon fibre-reinforced polymer/steel bonded joints. Advances in Science and Technology Research Journal. 2021;15(4):299–310. https://doi.org/10.12913/22998624/142370
4. Grund D., Orlishausen M., Taha I. Determination of fiber volume fraction of carbon fiber-reinforced polymer using thermogravimetric methods. Polym Test. 2019; 75: 358–366. https://doi.org/10.1016/j.polymertesting.2019.02.031
5. Voigt W. Ueber die Beziehung zwischen den beiden Elasticitätsconstanten isotroper Körper. Ann. Der Phys. 1889; 274: 573–587.
6. Reuss A. Calculation of the yield strength of mixed crystals due to the plasticity condition for single crystals. J. Appl. Math. Mech. 1929; 9: 49–58.
7. Mori T., Tanaka K. Average stress in matrix and average elastic energy of materials with misfitting inclusions. Acta Metall. 1973; 21: 571–574.
8. Bouchikhi A., Bakkali A., Abouelhanoune Y. Modeling of time and frequency dependent behavior of viscoelastic multi-layered reinforced composites with imperfect interfaces. Advances in Science and Technology Research Journal. 2025; 19(8): 44–67. https://doi.org/10.12913/22998624/204737
9. Skrzat A., Stachowicz F. Determination of effective properties of fiber-reinforced composite laminates. Advances in Science and Technology Research Journal. 2014; 8(22): 56–59. https://doi.org/10.12913/22998624.1105167
10. Kim Y.C., Jang H.-K., Joo G., Kim J.H. A comparative study of micromechanical analysis models for determining the effective properties of out-of-autoclave carbon fiber–epoxy composites. Polymers. 2024; 16: 1094. https://doi.org/10.3390/polym16081094
11. Aboudi J. Micromechanical analysis of composites by the method of cells. Appl. Mech. Rev. 1989; 42: 193–221.

12. Aboudi J., Arnold S.M., Bednarcyk B.A. Practical Micromechanics of Composite Materials; Butterworth-Heinemann: Oxford. UK. 2021.
13. Abaqus HTML Documentation
14. Wang W., Dai Y., Zhang C., Gao X., Zhao M. Micromechanical modeling of fiber-reinforced composites with statistically equivalent random fiber distribution. Materials. 2016; 9: 624. https://doi.org/10.3390/ma9080624
15. Shan M., Zhao L., Ye J. A Novel Micromechanics-Model-Based Probabilistic Analysis Method for the Elastic Properties of Unidirectional CFRP Composites. Materials. 2022; 15(15): 5090. https://doi.org/10.3390/ma15155090
16. Al Kassem G., Weichert D. Micromechanical material models for polymer composites through advanced numerical simulation techniques. Proceedings in applied mathematics and mechanics: PAMM. 2009; 9(1).
17. Kaddaha M.A., Younes R., Lafon P. Homogenization method to calculate the stiffness matrix of laminated composites. *Eng* 2021; *2*: 416–434. https://doi.org/10.3390/eng2040026
18. Katouzian M., Vlase S., Itu C., Scutaru M.L. Calculation of homogenized mechanical coefficients of fiber-reinforced composite using finite element method. *Materials* 2024; *17*: 1334. https://doi.org/10.3390/ma17061334
19. Jin J.-W., Jeon B.-W., Choi C.-W., Kang K.-W. Multi-scale probabilistic analysis for the mechanical properties of plain weave carbon/epoxy composites using the homogenization technique. *Appl. Sci.* 2020; *10*: 6542. https://doi.org/10.3390/app10186542
20. Huner U., Irsel G., Bekar U., Szala M. A comprehensive case study to the implicit and explicit approach in finite element analysis. Advances in Science and Technology Research Journal. 2025;19(2):407–17. https://doi.org/10.12913/22998624/196987
21. Trzepieciński T., Ryzińska G., Biglar M., Gromada M. Modelling of multilayer actuator layers by homogenization technique using Digimat software. Ceram. Int. 2016; 43: 3259–3266.
22. Frącz W., Janowski G. Influence of homogenization methods in prediction of strength properties for WPC composites. Applied Computer Science. 2017; 13(3): 77–89.
23. Frącz W., Janowski G., Ryzińska G. Strength analysis of GFRP composite product taking into account its het-erogenic structure for different reinforcements. Composites Theory and Practice. 2017; 17(2): 103–108.
24. Castelló-Pedrero P., García-Gascón C., García-Manrique J.A. Multiscale numerical modeling of large-format additive manufacturing processes using carbon fiber reinforced polymer for digital twin applications. Int J Mater. 2024; https://doi.org/10.1007/s12289-024-01811-5
25. Ryzińska G., Janowski G., Bąk Ł. Modeling of compression test of natural fiber composite sections. Advances in Science and Technology Research Journal. 2021; 15(2): 138–147. https://doi.org/10.12913/22998624/133486
26. Ryzińska G., Janowski G. Influence of rve geometrical parameters on elastic response of woven flax--epoxy composite materials. Composites Theory and Practice. 2020; 20(2): 51–59
27. Bastovansky R., Smetanka L., Kohar R. Mishra RK. Petru M. Comparison of mechanical property simulations with results of limited flexural tests of different multi-layer carbon fiber-reinforced polymer composites. *Polymers.* 2024; 16(11):1588. https://doi.org/10.3390/polym16111588
28. Dragicevic D., Schilling J.C., Mittelstedt C. Minimum stringer stiffness of shear deformable composite laminated plates for maximum buckling performance. Arch Appl Mech. 2025; 95: 211. https://doi.org/10.1007/s00419-025-02917-1
29. Gawryluk J., Głogowska K., Bartnicki H. Buckling of a structure made of a new eco-composite material. Applied Computer Science. 2025; 21(2): 28–36. https://doi.org/10.35784/acs_7308
30. Gawryluk J. The effect of fiber arrangement in the bio-laminate and geometric parameters on the stability of thin-walled angle column under axial compression. Advances in Science and Technology Research Journal. 2023;17(1):150–9. https://doi.org/10.12913/22998624/158854
31. Lu J., Zheng C., Wang L., Dai Y., Wang Z., Song Z. T700 carbon fiber/epoxy resin composite material hygrothermal aging model. *Materials.* 2025; 18(2):369. https://doi.org/10.3390/ma18020369
32. Jones R. Mechanics Of Composite Materials (2nd ed.). CRC Press. 2018
33. Altenbach H., Altenbach J., Kissing W. *Mechanics of Composite Structural Elements* (2nd ed.). Springer. 2018.
34. Budynas R. G., Nisbett J. K. *Shigley's Mechanical Engineering Design. 11th edition.* 2019.